temperature rate constant for the reaction of CH_3S with NO_2 of $\approx 1 \times 10^{-10}$ cm^3 molecule^{-1} s^{-1}. With $[NO_2] = 1.2 \times 10^{14}$ molecule cm^{-3} present in the study of MacLeod et al.,[15] the $[CH_3S]$ would be prohibitively small due to reaction with NO_2 to permit formation of DMDS by second-order recombination of CH_3S radicals. Therefore work on the primary products is clearly needed.

The atmospheric lifetimes of CH_3SH, C_2H_5SH, DMS, and DMDS, defined by reactions with NO_3 and OH, were compared by Atkinson et al.[14] and MacLeod et al.[15] They used $[OH] = 1 \times 10^6$ molecule cm^{-3} and $[NO_3] = 2 \times 10^8$ molecule cm^{-3}. The lifetimes (in hours) defined by reactions with OH were 8.4, 5.9, 44, and 1.3, respectively, and for NO_3, 1.2, 1.0, 1.2, and 28, respectively. Nighttime reactions of NO_3 with CH_3SH, C_2H_5SH, and DMS are reported to be the dominant loss processes for these species under these conditions. The only revision of their conclusions from our work is for CH_3SSCH_3. With our value for k_3 and the [OH] and $[NO_3]$ from above, the lifetime of DMDS due to reaction with NO_3 (1.6 h) is comparable with the lifetime due to reaction with OH (1.3 h). Based on our upper limits, reactions 4 and 5 are unimportant in the atmosphere relative to the corresponding reactions for OH.[41,42]

In summary, we have measured the rate constants for nitrate radical reactions with some important atmospheric sulfur species. Our results indicate that for reactions of NO_3 with DMS and CH_3SH, NO_2 is not a major product. We suggest that the reactions of NO_3 with DMS, CH_3SH, and DMDS are initiated by addition of NO_3 to the sulfur atoms. The fate of the NO_3 adduct has not been determined, but this will be important in determining the overall effect of these reactions on the atmospheric chemistry of the reduced sulfur species. Studies of the primary products of these reactions are warranted.

Acknowledgment. This work was supported by NOAA as part of the National Acid Precipitation Assessment Program. We thank G. Tyndall for many helpful comments on the manuscript.

Registry No. NO_3 radical, 12033-49-7; CH_3SCH_3, 75-18-3; CH_3SH, 74-93-1; CH_3SSCH_3, 624-92-0; H_2S, 7783-06-4; SO_2, 7446-09-5.

(40) Balla, R. J.; Nelson, H. H.; McDonald, J. R. *Chem. Phys.* **1986**, *109*, 101.

(41) $k(OH + H_2S) = 5 \times 10^{-12}$ cm^3 molecule^{-1} s^{-1}, DeMore, W. B.; Margitan, J. J.; Molina, M. J.; Watson, R. T.; Golden, D. M.; Hampson, R. F.; Kurylo, M. J.; Howard, C. J.; Ravishankara, A. R. "Chemical Kinetic and Photochemical Data for use in Stratospheric Modeling", NASA Panel for Data Evaluation; Evaluation No. 7; Jet Propulsion Laboratory Publication 85-37; 1985.

(42) Under atmospheric conditions: $T = 298$ K, $P = 1$ atm, $k(OH + SO_2) = 9 \times 10^{-13}$ cm^3 molecule^{-1} s^{-1}. Davis, D. D.; Ravishankara, A. R.; Fischer, S. *Geophys. Res. Lett.* **1979**, *6*, 113.

Kinetics of the Reaction OH + HO_2 → H_2O + O_2 from 254 to 382 K

Leon F. Keyser

Jet Propulsion Laboratory, California Institute of Technology, Pasadena, California 91109
(Received: June 30, 1987; In Final Form: September 8, 1987)

The discharge-flow resonance fluorescence technique has been used to determine the absolute rate constant for the reaction OH + HO_2 → H_2O + O_2 from 254 to 382 K at a total pressure of 1 Torr. Pseudo-first-order conditions were used with HO_2 in large excess over OH. The rate constant was obtained directly from observed decays of OH and measured concentrations of HO_2. Since the observed rate constant was found to be very sensitive to small background concentrations of O and H atoms, NO_2 was used to remove both atom species from the system. With added NO_2 the result at 299 K is $(1.1 \pm 0.3) \times 10^{-10}$ cm^3 molecule^{-1} s^{-1} where the error limits are one standard deviation and include an estimate of overall experimental uncertainty. The temperature dependence expressed in Arrhenius form is $(4.8 \pm 0.8) \times 10^{-11} \exp[(250 \pm 50)/T]$. The results are independent of the type of reactor surface and the precursor used to produce OH and HO_2. The present results agree well with earlier measurements near 1-atm total pressure and suggest that this rate constant exhibits little or no pressure dependence between 1 and 1000 Torr.

Introduction

In the upper atmosphere, HO_x radicals (H, OH, HO_2) enter several catalytic cycles which destroy odd oxygen (O, O_3). HO_x also interact with other radical families such as NO_x and ClO_x. From about 25 to 80 km the reaction of OH with HO_2 (eq 1) is

$$OH + HO_2 \rightarrow H_2O + O_2 \qquad (1)$$

a major loss of HO_x. As such, it plays a central role in determining the absolute concentrations of both OH and HO_2 over this region and, thus, limits the efficiency with which they remove odd oxygen and the extent to which they influence other trace radical species.[1-7]

Many early measurements of this rate constant were indirect and resulted in much disagreement. In recent years there have been several more direct measurements. At low pressure the data were obtained by the discharge-flow technique mostly near 2 Torr with a limited number of observations as high as 10 Torr. These recent results are in good agreement and near 300 K yield an average value of $(6.6 \pm 1.5) \times 10^{-11}$ cm^3 molecule^{-1} s^{-1} for k_1.[8-12] The high-pressure data were obtained by photolysis experiments mostly above 700 Torr. These results agree among themselves and yield for k_1 an average value of $(12 \pm 4) \times 10^{-11}$ cm^3 mol-

(1) Clancy, R. T.; Rusch, D. W.; Thomas, R. J.; Allen, M.; Eckman, R. S. *J. Geophys. Res.* **1987**, *92*, 3067.
(2) Natarajan, M.; Callis, L. B.; Boughner, R. E.; Russell, J. M. III; Lambeth, J. D. *J. Geophy. Res.* **1986**, *91*, 1153.
(3) Kaye, J. A.; Jackman, C. H. *J. Geophys. Res.* **1986**, *91*, 1117.
(4) Rusch, D. W.; Eckman, R. S. *J. Geophys. Res.* **1985**, *90*, 12991.
(5) "Atmospheric Ozone 1985: Assessment of our Understanding of the Processes Controlling Its Present Distribution and Change, WMO Global Ozone Research and Monitoring Project, Report No. 16"; National Aeronautics and Space Administration: Washington, D.C., 1986.
(6) Allen, M.; Lunine, J. I.; Yung, Y. L. *J. Geophys. Res.* **1984**, *89*, 4841.
(7) "The Stratosphere 1981: Theory and Measurements, WMO Global Ozone Research and Monitoring Project, Report No. 11"; Hudson, R., Ed.; World Meteorological Organization: Geneva, Switzerland, 1982.
(8) Sridharan, U. C.; Qiu, L. X.; Kaufman, F. *J. Phys. Chem.* **1984**, *88*, 1281.
(9) Sridharan, U. C.; Qiu, L. X.; Kaufman, F. *J. Phys. Chem.* **1981**, *85*, 3361.
(10) Temps, F.; Wagner, H. Gg. *Ber. Bunsen-Ges. Phys. Chem.* **1982**, *86*, 119.
(11) Thrush, B. A.; Wilkinson, J. P. T. *Chem. Phys. Lett.* **1981**, *81*, 1.
(12) Keyser, L. F. *J. Phys. Chem.* **1981**, *85*, 3667.

0022-3654/88/2092-1193$01.50/0

ecule^{-1} s^{-1},[13-19] which may be significantly higher than the low-pressure result. In a recent study, DeMore reports an increase in k_1 from 7×10^{-11} at 75 Torr to 12×10^{-11} cm^3 molecule^{-1} s^{-1} at 730 Torr.[13] The difference between the low- and high-pressure results along with DeMore's observations suggests that a pressure-dependent third-order component may contribute to the observed loss of OH by reaction with HO_2.

Data on the temperature dependence of this reaction are extremely limited. The only low-pressure study gives a negative Arrhenius activation energy of 0.8 kcal mol^{-1}.[8] However, at high pressure the only study gives a temperature-independent rate constant over a limited temperature range.[15]

This rate constant is extremely difficult to measure since it requires the preparation of two highly reactive radical species plus the determination of the absolute concentration of one in order to obtain an absolute rate coefficient. Since for the present study HO_2 is best generated from H_2O_2 (cf. below), there is always a background loss of OH due to reaction with H_2O_2 (eq 2).

$$OH + H_2O_2 \rightarrow HO_2 + H_2O \quad (2)$$

Moreover, both radicals disproportionate: HO_2 gives H_2O_2 (eq 3, $k_3 = 1.7 \times 10^{-12}$) while OH gives O atoms (eq 4, $k_4 = 1.9 \times 10^{-12}$) which in turn react with OH to produce H atoms (eq 5, $k_5 = 3.3 \times 10^{-11}$). All rate constants are in units of cm^3 molecule^{-1} s^{-1}. Because of reactions 4 and 5, it is not possible to prepare OH without also generating some O and H atoms, both of which react with HO_2 to generate OH (eq 6, $k_6 = 6.1 \times 10^{-11}$; eq 7a, $k_{7a} = 7.8 \times 10^{-11}$). Reactions 6 and 7a can interfere with measurements

$$HO_2 + HO_2 \rightarrow H_2O_2 + O_2 \quad (3)$$

$$OH + OH \rightarrow O + H_2O \quad (4)$$

$$O + OH \rightarrow H + O_2 \quad (5)$$

$$O + HO_2 \rightarrow OH + O_2 \quad (6)$$

$$H + HO_2 \rightarrow OH + OH \quad (7a)$$

of OH decay rates if O or H atom concentrations are sufficiently high. This was recognized in earlier studies of this rate constant. However, recent determinations of k_6[20-23] and k_7[22,24] have resulted in values which are 2–6 times larger than previously accepted. Thus, the OH + HO_2 rate constant measurements are considerably more sensitive to O and H atoms than previously thought.

The goals of the present study are to determine the temperature dependence of k_1 and to search for a possible pressure effect. Pseudo-first-order conditions are used with [HO_2] in large excess over [OH]. The rate constant is obtained directly from the observed decays of OH. The sensitivity of the measured rate constant to atomic species is checked by addition of known concentrations of O and H atoms. An atom scavenger is also added to reduce the interference from reactions 6 and 7a.

Experimental Method

Low-Pressure Flow System. The discharge-flow system and dual resonance fluorescence detector have been described in detail previously.[23,25] The present study utilized a 50.4-mm-diameter reactor coated with halocarbon wax. For some measurements a 43.2-mm-diameter Teflon (poly(tetrafluoroethylene)) liner was used to check for wall reactions. The surface condition was monitored by measuring the OH wall loss rate, k_w, following each series of runs. Without added NO k_w ranged from approximately 1 to 11 s^{-1}. Similar results were obtained for the wax-coated and Teflon surfaces. Previous measurements of k_w for HO_2, O, and H showed that on wax-coated surfaces in this same reactor their loss rates were less than 5 s^{-1}.[24] Calibrated mass flowmeters were used to measure all flow rates except $NO_2 + O_2$ mixtures for which the pressure drop in a calibrated volume was used. Pressures were measured by using calibrated capacitance monometers.

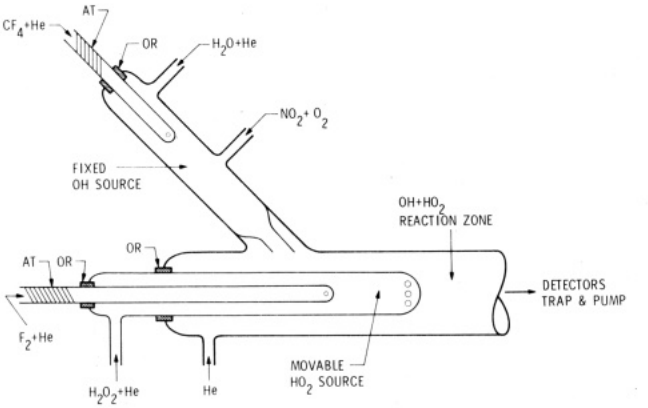

Figure 1. Schematic drawing of the discharge-flow system used in the present measurements. AT = alumina tube, site of 2.45-GHz discharge; OR = O-ring seal.

OH Production and Detection. OH was produced in a fixed source at the upstream end of the OH + HO_2 reaction zone by adding F atoms to an excess of H_2O vapor (eq 8). The F atoms

$$F + H_2O \rightarrow OH + HF \quad (8)$$

were generated in a 2.45-GHz discharge of CF_4 or F_2 in helium. Figure 1 shows the fixed OH source and its position relative to the movable HO_2 source and the OH + HO_2 reaction zone. All surfaces except the alumina discharge tube were coated with halocarbon wax. A total flow rate near 660 cm^3 min^{-1} (STP) at a source pressure of 1.8 Torr resulted in approximately a 12-ms residence time in the 25-mm-i.d. source. Between the OH source exit and the addition point of HO_2, the OH radicals passed through a ring-shaped region formed by the inner surface of the main reactor and the outer wall of the movable HO_2 source; the transit time through this region was approximately 55 ms. The concentration ratio between the source and the main reactor was 6.5; between the ring-shaped region and the main reactor it was 1.6. Typical concentrations in the main reactor were [OH] = 1.3×10^{11} cm^{-3} with background [O] = 8×10^9 and [H] = 1.5×10^{10} cm^{-3}. Production efficiencies were near 50% with F_2 and 30% with CF_4 as the source of F atoms.

In some experiments known concentrations of O or H atoms were added to the reaction mixture in order to check the sensitivity of observed values of k_1 to these species. These atoms were generated in a separate microwave discharge of either O_2 or H_2 in helium and added to OH at the OH source exit. Atom concentrations in the range 2×10^{10} to 7×10^{10} cm^{-3} were added.

For most of the present experiments NO_2 was added to scavenge background O and H atoms and thus reduce interference from reactions 6 and 7a. NO_2 reacts with both atom species to form NO (eq 9 and 10). An excess of NO_2 was added to the OH source

$$O + NO_2 \rightarrow O_2 + NO \quad (9)$$

$$H + NO_2 \rightarrow OH + NO \quad (10)$$

approximately 5 ms after the start of the F + H_2O reaction (eq

(13) DeMore, W. B. *J. Phys. Chem.* **1982**, *86*, 121.
(14) Braun, M.; Hofzumahaus, A.; Stuhl, F. *Ber. Bunsen-Ges. Phys. Chem.* **1982**, *86*, 597.
(15) Burrows, J. P.; Cox, R. A.; Derwent, R. F. *J. Photochem.* **1981**, *16*, 147.
(16) Cox, R. A.; Burrows, J. P.; Wallington, T. J. *Chem. Phys. Lett.* **1981**, *84*, 217.
(17) Kurylo, M. J.; Klais, O.; Laufer, A. H. *J. Phys. Chem.* **1981**, *85*, 3674.
(18) Hochandel, C. J.; Sworski, T. J.; Ogren, P. J. *J. Phys. Chem.* **1980**, *84*, 3274.
(19) Lii, R. R.; Gorse, R. A., Jr.; Sauer, M. C.; Gordon, S. *J. Phys. Chem.* **1980**, *84*, 819.
(20) Brune, W. H.; Schwab, J. J.; Anderson, J. G. *J. Phys. Chem.* **1983**, *87*, 4503.
(21) Ravishankara, A. R.; Wine, P. H.; Nicovich, J. M. *J. Chem. Phys.* **1983**, *78*, 6629.
(22) Sridharan, U. C.; Qiu, L. X.; Kaufman, F. *J. Phys. Chem.* **1982**, *86*, 4569.
(23) Keyser, L. F. *J. Phys. Chem.* **1982**, *86*, 3439.
(24) Keyser, L. F. *J. Phys. Chem.* **1986**, *90*, 2994.
(25) Keyser, L. F.; Choo, K. Y.; Leu, M. T. *Int. J. Chem. Kinet.* **1985**, *17*, 1169.

8). Like O and H atoms, NO reacts with HO_2 to form OH (eq 11, $k_{11} = 8.3 \times 10^{-12}$) but with a rate coefficient approximately

$$NO + HO_2 \rightarrow OH + NO_2 \quad (11)$$

10 times lower. Thus, conversion of atoms to NO can reduce considerably the interference from reactions 6 and 7a. To prevent any significant interference from reaction 11, the rate of OH production by this reaction should be kept less than about 10–20% of the OH loss rate by reaction 1; that is, $k_{11}[NO]_0 \cdot \exp(-k_{11}[HO_2]t) < 0.1k_1[OH]_0 \exp(-k_1[HO_2]t)$. For reaction times of 10–15 ms and a typical HO_2 concentration of 2×10^{12} cm^{-3}, this means that $[NO]_0 = [O]_0 + [H]_0$ should be about 5–10 times lower than $[OH]_0$. Thus, NO_2 can be used to scavenge O and H atoms only if initial concentrations of these atoms are relatively low compared to initial OH. It should also be noted that the H + NO_2 reaction (eq 10) cannot be used as a source of OH in the present experiments because then $[NO]_0$ would equal $[OH]_0$ and reaction 11 would interfere strongly. With NO_2 added, atom concentrations were very low and thus difficult to measure accurately. For typical conditions with $[NO_2] = 1.0 \times 10^{13}$ and $[OH] = 1.3 \times 10^{11}$ cm^{-3}, [O] averaged less than 1×10^9 cm^{-3} and [H] averaged less than about 3×10^9 cm^{-3} in the main reactor.

Detector Calibrations. OH was monitored by resonance fluorescence near 308 nm. Known concentrations were generated by reacting NO_2 with excess H atoms (eq 10). Calibrations were run at OH concentrations corresponding to the concentrations of OH and HO_2 observed during the experimental runs. Corrections were made for OH loss at the wall and disproportionation (eq 4) by using measured values of OH decay. These corrections were made only up to the NO addition port. Downstream similar losses are present in both the OH calibration and the HO_2 to OH conversion and tend to cancel.[23] The fluorescence signal was linear within 5% for $[OH] < 1 \times 10^{12}$ cm^{-3}.

Atomic oxygen was followed by resonance fluorescence near 130 nm. Oxygen atom concentrations were calibrated by adding a known amount of NO to an excess of N atoms. Atomic hydrogen concentrations were monitored by resonance fluorescence at 121.6 nm and calibrated by converting the atomic hydrogen to OH by adding an excess of NO_2 (eq 10).[24]

HO_2 Production and Detection. The HO_2 source was similar to one described in detail previously.[12] HO_2 radicals were generated in a movable reactor by adding atomic fluorine to an excess of H_2O_2 (eq 12). Atomic fluorine was produced in a microwave

$$F + H_2O_2 \rightarrow HO_2 + HF \quad (12)$$

discharge of dilute mixtures of either F_2 or CF_4 in helium. In both cases an uncoated alumina discharge tube was used with power levels at 10–20 W. Typical production efficiencies were 20% with F_2 and 0.2% with CF_4. This source was used to generate HO_2 at concentrations between 6×10^{11} and 4×10^{12} cm^{-3} in the main reaction zone. Background concentrations of OH were less than 1×10^{10} cm^{-3} with both O and H atoms less than 2×10^9 cm^{-3}. Other sources of HO_2 such as H + O_2 + M or CH_2OH + O_2 are not suitable for the present study because of low production efficiency or interference from products. Concentrations of HO_2 were determined by quantitatively converting it to OH with an excess of NO (eq 11) which was added 1.5–4.5 ms upstream of the OH detector. Details of this method and the corrections for radical losses which are necessary to obtain absolute HO_2 concentrations have been discussed earlier.[23]

Reagents. Gases used were chromatographic grade helium (99.9999%), research grade hydrogen (99.9995%), ultrahigh-purity oxygen (99.98%), ultrahigh-purity nitrogen (99.999%), nitric oxide (99.0%), CF_4 (99.9%), and 0.5% or 5.0% mixtures of F_2 in helium. The nitric oxide was purified by passage through a molecular sieve (13X) trap at 195 K. The fluorine in helium mixtures were passed through a molecular sieve (3A) trap at 77 K just prior to use. Hydrogen peroxide was obtained commercially and concentrated further by vacuum distillation. Vapor pressure measurements indicated that the final liquid-phase concentration was 96 wt %. Water vapor was added to the reaction mixture by passing a stream of helium through the liquid which was maintained at a constant temperature. Nitrogen dioxide used to calibrate the OH detector was prepared from nitric oxide as described earlier.[23] The NO_2 used to scavenge O and H atoms was also prepared from NO by adding excess O_2. However, in this case the O_2 was not removed and the NO_2 was stored and added to the flow tube as a mixture of NO_2 (N_2O_4) and O_2 in order to minimize NO. Typical conditions were 500 Torr of initial NO and enough O_2 to bring the final pressure to about 760 Torr. The NO_2 + O_2 mixture was added from a calibrated volume held at constant temperature.

Results

Experimental Conditions. Concentrations of HO_2 were in the range 6×10^{11} to 4×10^{12} cm^{-3} with initial OH from 6×10^{10} to 2×10^{11} cm^{-3}. Initial stoichiometric ratios ranged from 7 to 25 and averaged greater than 13. Concentrations of H_2O_2 were between 1.4×10^{13} and 3×10^{13} cm^{-3} with NO_2 near 1×10^{13} cm^{-3}. Temperatures were in the range 254–382 K at a total pressure of 1 Torr of helium.

Data Analysis. Under these conditions, the loss of OH is pseudo-first-order. With HO_2 added to the system (movable discharge on), the loss may be written

$$-\mathrm{d} \ln [OH]_+/\mathrm{d}t = k_1^+ = k_1[HO_2] + k_2[H_2O_2] + k_L \quad (I)$$

where k_L represents loss of OH other than by reaction with HO_2 or H_2O_2. It would, for example, include possible secondary reactions with species added or produced in the movable HO_2 source. Without HO_2 (movable discharge off), the loss of OH is

$$-\mathrm{d} \ln [OH]_-/\mathrm{d}t = k_1^- = k_2[H_2O_2] + k_L' \quad (II)$$

One experimental run consists of a pair of OH loss measurements to determine both k_1^+ and k_1^- under similar conditions. The difference between the two decay rates ($k_1^+ - k_1^-$) and a measurement of the absolute concentration of HO_2 yield k_1 (eq III).

$$k_1 = (k_1^+ - k_1^-)/[HO_2] \quad (III)$$

This assumes that OH losses due to secondary reactions are small or do not change appreciably, $(k_L - k_L') \ll k_1[HO_2]$, when the HO_2 source is switched on and off. Evidence that the secondary chemistry is unimportant is provided by using two different F atom precursors in the HO_2 source and will be discussed below.

Observed first-order rate constants were corrected for axial and radial diffusion (less than 15%) by using a method described previously.[26,27] For these corrections a value of 752 cm^2 s^{-1} was used for the diffusion coefficient of OH in He at 300 K and 1 Torr; a temperature dependence of $T^{1.5}$ was used to estimate the diffusion coefficient at the other temperatures.[27] Corrections due to the viscous pressure drop between the center of the reaction zone and the pressure measurement port were less than 1%.[28]

Equation II neglects loss of OH due to reaction with the small amount of HO_2 formed by reaction of OH with H_2O_2 (eq 2). Computer simulations were used to estimate this loss, and corrections typically less than 3% were applied to ($k_1^+ - k_1^-$).

Equation III assumes that $[H_2O_2]$ is the same with and without added HO_2. However, some H_2O_2 is consumed in the HO_2 source mainly by reaction with F (eq 12) and OH (eq 2); corrections averaging about 3% have been applied to ($k_1^+ - k_1^-$) for this H_2O_2 loss. These corrections were derived from computer simulations of the HO_2 source.

Corrections averaging less than 10% have been applied to ($k_1^+ - k_1^-$) to account for OH production from reaction 11 when NO_2 was added. These corrections were based on computer simulations of the OH + HO_2 reaction and are discussed below.

Concentrations of HO_2 were determined by averaging the values observed at the minimum and maximum reaction times. The total observed HO_2 decays due to wall loss, disproportionation (eq 3),

(26) Brown, R. L. *J. Res. Natl. Bur. Stand. (U.S.)* **1978**, *83*, 1.
(27) Keyser, L. F. *J. Phys. Chem.* **1984**, *88*, 4750.
(28) Kaufman, F. *Prog. React. Kinet.* **1961**, *1*, 1.

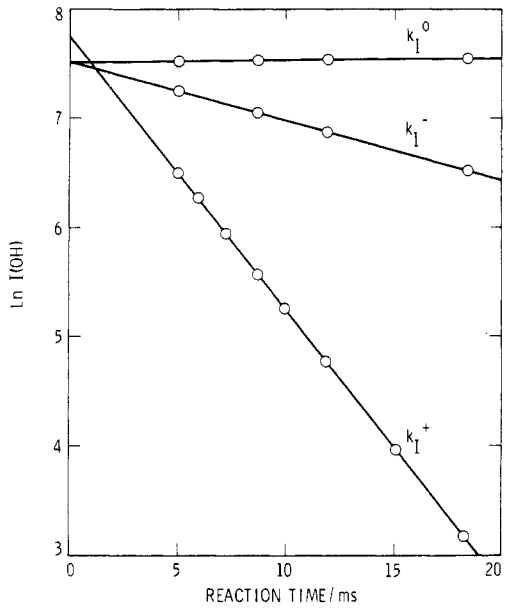

Figure 2. OH decay curves at 273 K: in the absence of both H_2O_2 and HO_2 (k_I^0); with H_2O_2 added (k_I^-); and with both H_2O_2 and HO_2 added (k_I^+). $[OH]_0 = 1.7 \times 10^{11}$, $[HO_2] = 2.3 \times 10^{12}$, $[H_2O_2] = 2.3 \times 10^{13}$, and $[NO_2] = 1.1 \times 10^{13}$ cm^{-3}.

and reaction with OH were typically less than about 15% except at 382 K were the losses were generally 20–45%. Corrections (less than 20%) for radical losses during the HO_2 to OH conversion have been applied to the observed HO_2 concentrations.[23]

The largest corrections are due to diffusion, to OH production from reaction 11, and to loss of HO_2 during the conversion to OH. The first two corrections act to increase the value of k_1 while the third decreases it; thus, their net effect is relatively small. Correction for the viscous pressure drop acts to decrease k_1 while the remaining corrections increase k_1, but these are all small in magnitude. The net effect of all these corrections is to increase the observed value of k_1 by less than 16%, which is well within the estimated experimental uncertainty of ±25%.

Summary of Results. Typical OH decay curves at 273 K are shown in Figure 2 where the three curves represent OH loss in the absence of both H_2O_2 and HO_2 (k_I^0), with H_2O_2 added (k_I^-), and with both H_2O_2 and HO_2 added (k_I^+). The k_I^0 curve is not used in the rate constant measurement; it is shown only to demonstrate that there is no major OH loss due to reaction with undissociated F_2 or CF_4 present in the HO_2 source or with reaction products formed by the interaction of these species with the OH source. Generally, no curvature was observed in k_I^+ or k_I^- plots over the 5–18-ms time interval used. However, some k_I^+ plots showed negative curvature (lower slope) at long reaction times; in these cases, the initial slope was used to calculate the OH decay.

Table I summarizes the rate constant measurements with added NO_2. All entries have been corrected as discussed in the data analysis section above. The last column gives the values for the bimolecular rate constant, k_1, obtained from $(k_I^+ - k_I^-)/[HO_2]$. Values for k_1 were also calculated from the slopes of $(k_I^+ - k_I^-)$ vs $[HO_2]$ plots, and the results are compared in Table II. Values of k_1 obtained by averaging the individual measurements of $(k_I^+ - k_I^-)/[HO_2]$ (column 2) agree within one standard deviation with those obtained from the slopes (column 3). The results reported for the present measurements were obtained from the averages. At 299 K $k_1 = (10.8 \pm 1.0) \times 10^{-11}$ cm^3 molecule^{-1} s^{-1} where the error limits are one standard deviation obtained from the data analysis; overall experimental error is estimated to be ±25%. The data are plotted in Arrhenius form in Figure 3. The resulting Arrhenius expression obtained from an unweighted linear least-squares analysis of the data is

$$k_1 \text{ (cm}^3 \text{ molecule}^{-1} \text{ s}^{-1}) = (4.8 \pm 0.8) \times 10^{-11} \exp[(250 \pm 50)/T]$$

for $254 \le T \le 382$ K. The errors given in the above expression

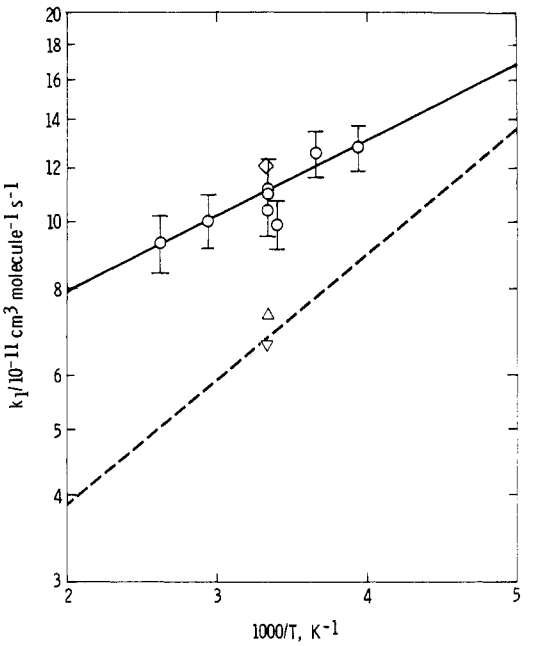

Figure 3. Arrhenius plot of the rate data for OH + HO_2: ○, present results with added NO_2 scavenger; △, present results without added NO_2; ▽, average of previous low-pressure measurements; ◇, average of previous high-pressure measurements. The error bars are one standard deviation. The solid line is the Arrhenius fit to the present data. The dashed line is the Arrhenius fit to the only previous study of the temperature dependence at low pressures.[8]

and in Figure 3 are one standard deviation. The temperature dependence is significant at the 67% confidence level (one standard deviation); however, at the 95% level (two standard deviations) the data can be fit by a temperature-independent average value of $(10.8 \pm 2.8) \times 10^{-11}$ cm^3 molecule^{-1} s^{-1}.

The results without added NO_2 are summarized in Figure 4. For some of these experiments the O and H atoms present were generated mainly in the OH source, either in the discharge itself or by reactions 4 and 5. Typical values were $[O] = 8 \times 10^9$ and $[H] = 1.5 \times 10^{10}$ cm^{-3}. In some experiments atom concentrations were determined immediately following the k_1 measurements (filled points); in other experiments concentrations were determined only at the end of a series of runs (open points). The considerable scatter in the data may be due to variations in background atom concentrations; thus, higher weight is given to the filled data points which represent better controlled experiments. Without added NO_2 the average observed k_1 is $(7.3 \pm 1.0) \times 10^{-11}$ cm^3 molecule^{-1} s^{-1}, which agrees well with the 6.6×10^{-11} average of previous low-pressure measurements of k_1.[8-12]

In other experiments additional O and H atoms at concentrations between 2×10^{10} and 7×10^{10} cm^{-3} were introduced into the reaction mixture. The sensitivity of observed k_1 to O and H atom interference is seen in Figure 4. The line is the result of a computer simulation and will be discussed below.

Discussion

Secondary Chemistry and Systematic Errors. To check for possible interference from secondary reactions, CF_4 and F_2 were used to generate atomic fluorine in both the OH and HO_2 sources. No significant difference was observed in k_1 by using various combinations of these F atom precursors (see Tables I and II); this is evidence that there is negligible OH loss due to reaction with impurities produced in the sources.

At all temperatures studied, nonzero intercepts were observed in the $(k_I^+ - k_I^-)$ vs $[HO_2]$ plots (Table II, column 4). This can be interpreted as a change in surface loss of OH when HO_2 is added to the system (movable discharge on).[29] If this is the case, the slopes should be used to estimate k_1. However, the observed intercepts all lie within one standard deviation of the origin and,

(29) Westenberg, A. A.; de Haas, N. *J. Chem. Phys.* **1967**, *46*, 490.

TABLE I: Rate Constant Data for OH + HO_2[a]

$10^{-12}[HO_2]_0$, cm^{-3}	$10^{-11}[OH]_0$, cm^{-3}	$(k_1^+ - k_1^-)$, s^{-1}	$10^{11}k_1$, cm^3 $molecule^{-1}$ s^{-1}
T = 254 K, v = 1454 cm s^{-1}, OH from CF_4, HO_2 from F_2[b]			
0.959	1.03	118	12.3
1.24	1.17	153	12.3
1.50	1.41	187	12.5
1.76	1.58	261	14.8
2.27	1.59	297	13.1
2.58	1.34	306	11.9
			av = 12.8 ± 1.0[c]
T = 273 K, v = 1541 cm s^{-1}, OH from CF_4, HO_2 from F_2[b]			
0.864	0.68	111	12.8
1.08	1.24	134	12.4
1.57	1.07	184	11.7
1.65	1.86	234	14.2
2.26	1.68	273	12.1
2.73	2.02	325	11.9
			av = 12.5 ± 0.9[c]
T = 294 K,[d] v = 1830 cm s^{-1}, OH from CF_4, HO_2 from F_2[b]			
0.794	1.20	75.3	9.48
1.04	1.21	101	9.71
1.33	1.44	125	9.40
1.68	1.42	164	9.76
2.22	1.52	253	11.4
3.07	1.75	289	9.41
			av = 9.9 ± 0.8[c]
T = 299 K, v = 1710 cm s^{-1}, OH from CF_4, HO_2 from F_2[b]			
0.892	0.81	91.3	10.2
1.05	1.29	131	12.5
1.40	1.69	151	10.8
1.54	1.32	153	9.94
1.63	1.16	163	10.0
1.76	1.61	219	12.4
2.00	1.23	189	9.45
2.52	1.70	292	11.6
2.63	1.38	288	11.0
2.81	1.74	329	11.7
			av = 11.0 ± 1.1[c]
T = 299 K, v = 1690 cm s^{-1}, OH from F_2, HO_2 from F_2[b]			
1.14	0.92	129	11.3
1.19	1.24	109	9.16
1.27	1.43	138	10.9
1.57	1.23	175	11.2
2.24	1.52	254	11.3
2.51	1.33	215	8.57
2.79	1.55	287	10.3
3.14	1.26	337	10.7
3.40	1.48	362	10.6
3.83	1.63	399	10.4
			av = 10.4 ± 0.9[c]
T = 299 K, v = 1695 cm s^{-1}, OH from CF_4, HO_2 from CF_4[b]			
0.787	0.70	79.3	10.1
0.900	0.64	115	12.8
1.04	0.68	113	10.9
1.37	0.64	147	10.7
			av = 11.1 ± 1.2[c]
T = 340 K, v = 1700 cm s^{-1}, OH from CF_4, HO_2 from F_2[b]			
0.807	0.99	69.6	8.62
1.05	0.98	116	11.0
1.26	1.12	118	9.36
1.65	1.56	180	10.9
2.06	1.25	203	9.85
2.58	1.16	266	10.3
			av = 10.0 ± 0.9[c]
T = 382 K, v = 1695 cm s^{-1}, OH from CF_4, HO_2 from F_2[b]			
0.650	0.82	61.8	9.51
0.921	0.75	80.2	8.71
1.05	1.48	106	10.1
1.36	0.91	139	10.2
1.73	1.36	161	9.31
2.01	1.24	156	7.76
			av = 9.3 ± 0.9[c]

[a] Total pressure was 1.0 Torr of helium with $[NO_2]$ = 1.0 × 10^{13} cm^{-3}, and unless otherwise indicated the experiments were carried out in a 50.4-mm-diameter reactor coated with halocarbon wax. [b] OH was produced from the F + H_2O reaction and HO_2 from the F + H_2O_2 reaction by using the F atom precursors indicated. [c] Errors given are one standard deviation. [d] These experiments were carried out in a reactor lined with a 43.2-mm-diameter Teflon (poly(tetrafluoroethylene)) tube.

TABLE II: Rate Constants for the OH + HO_2 Reaction[a]

temp, K	$10^{11}k_1$, cm^3 $molecule^{-1}$ s^{-1} average[b,c]	slope[b,d]	intercept[b,d]
254	12.8 ± 1.0	12.4 ± 1.6	8 ± 29
273	12.5 ± 0.9	11.5 ± 1.0	15 ± 19
294[e]	9.9 ± 0.8	10.0 ± 1.0	−1 ± 18
299	11.0 ± 1.1	11.6 ± 1.0	−12 ± 18
299[f]	10.4 ± 0.9	10.4 ± 0.7	1 ± 17
299[g]	11.1 ± 1.2	10.2 ± 2.8	9 ± 30
340	10.0 ± 0.9	10.6 ± 0.8	−7 ± 13
382	9.3 ± 0.9	7.6 ± 1.2	19 ± 17

[a] Unless otherwise indicated, the experiments were carried out in a 50.4-mm-diameter reactor coated with halocarbon wax. OH was produced from the F + H_2O reaction by using CF_4 as the F atom precursor; HO_2 was produced from the F + H_2O_2 reaction by using F_2 as the precursor. [b] Errors given are one standard deviation. [c] From average of individual $(k_1^+ - k_1^-)/[HO_2]$ values. [d] From plot of $(k_1^+ - k_1^-)$ vs $[HO_2]$. [e] These experiments were carried out in a reactor lined with a 43.2-mm-diameter Teflon tube. [f] F_2 was F atom precursor for production of both OH and HO_2. [g] CF_4 was F atom precursor for production of both OH and HO_2.

as pointed out above, the rate constants calculated from the slopes agree within one standard deviation with the values obtained from the averages (compare columns 2 and 3 of Table II). Thus, there does not appear to be any significant surface loss of OH in this system. As an experimental check, several k_1 measurements were carried out at a slightly higher surface-to-volume ratio by using a Teflon liner in the flow reactor. The results, shown in Tables I and II, do not differ significantly and confirm the absence of interference from OH surface reactions.

Most of the present experiments were carried out in the presence of NO_2 at 1.0 × 10^{13} cm^{-3}. At this concentration losses of OH due to reactions with species formed by the NO_2 chemistry are not expected to interfere. Both OH and HO_2 combine with NO_2 (eq 13 and 14; k_{13} = 9.2 × 10^{-31} and k_{14} = 1.0 × 10^{-31} cm^6 $molecule^{-2}$ s^{-1}) and OH reacts with the products of both these

$$OH + NO_2 + He \rightarrow HONO_2 + He \quad (13)$$

$$HO_2 + NO_2 + He \rightarrow HO_2NO_2 + He \quad (14)$$

reactions (eq 15 and 16, k_{15} = 1.0 × 10^{-13} and k_{16} = 4.6 × 10^{-12} cm^3 $molecule^{-1}$ s^{-1}). Estimates using the above rate constants

$$OH + HONO_2 \rightarrow H_2O + NO_3 \quad (15)$$

$$OH + HO_2NO_2 \rightarrow \text{products} \quad (16)$$

with average concentrations and contact times show that these reactions do not constitute a significant loss of OH in the present study. This is confirmed by computer simulations of the system discussed below.

To check the flowmeter, pressure gauge, and detector calibrations used in the present study, the rate constant for the reaction of atomic oxygen with HO_2 (eq 6) was redetermined. The average of five runs at 299 K yields a value of (6.3 ± 0.4) × 10^{-11} cm^3 $molecule^{-1}$ s^{-1} for k_6, which is in excellent agreement with the value of (6.1 ± 0.4) × 10^{-11} obtained earlier in this laboratory.[23] This result confirms that there are no large systematic differences

between the earlier calibrations and those used in the present measurements.

Computer Simulations. Various aspects of the present study were simulated by using a numerical model based on the reactions and rate constants listed in Table III. The main purpose of these simulations was to obtain correction factors needed to analyze the data and to check for possible interference from secondary chemistry.

As described in detail earlier,[23] both the OH calibration and the conversion of HO_2 to OH with excess NO were simulated to estimate radical losses in both processes. The results were used to correct observed HO_2 concentrations; the size of these corrections averaged less than 15%. Simulations were also used to obtain corrections for OH loss by reaction with HO_2 formed from $OH + H_2O_2$ and for loss of H_2O_2 in the HO_2 source (see above); these small corrections were typically about 3%.

Computer simulations were also used to assess the influence of secondary chemistry on observed values of k_1. For this purpose the $OH + HO_2$ reaction was modeled by using initial concentrations of OH, HO_2, O, and H close to those observed in experimental runs. Values of k_1 were obtained by analyzing the model output in a manner identical with that used for the experimental data. Simulations were run both with and without added NO_2. The results without NO_2 are plotted in Figure 4, which illustrates the sensitivity of observed k_1 to relatively small concentrations of O and H atoms. The agreement between observation and calculation is remarkably good since no adjustable parameters were used. Both experiments and models show that background O and H atoms can lower significantly the observed rate constant.

With NO_2 present the values of k_1 calculated from the model are lower than the input value used, but this difference is much less than without the added scavenger. This apparent rate constant lowering depends on the concentrations of both HO_2 and H_2O_2. At typical concentrations of $[OH]_0 = 1.5 \times 10^{11}$, $[O]_0 = 8 \times 10^9$, $[H]_0 = 1.4 \times 10^{10}$, $[H_2O_2] = 2.5 \times 10^{13}$, and $[NO_2]_0 = 1.0 \times 10^{13}$ cm^{-3}, k_1 obtained from the model is lower than the input value by 5%, 12%, and 19% for $[HO_2] = 1 \times 10^{12}$, 2×10^{12}, and 3×10^{12} cm^{-3}, respectively. This residual lowering of k_1 is due mainly to regeneration of OH from the reaction of NO with HO_2 (eq 11). The NO was formed as a product of the reaction of NO_2 with O and H atoms (eq 9 and 10). Corrections based on these simulations have been applied to the $(k_1^+ - k_1^-)$ values reported here. The size of these corrections averaged about 10%.

Comparison with Previous Results. In Table IV the present results are compared with recent measurements of k_1 at low pressure. Four of these studies,[8-10,12] including the present study, were absolute measurements in which k_1 was obtained from observed OH decays and concentrations of HO_2 which was present in excess. Near 300 K these results average $(6.8 \pm 0.8) \times 10^{-11}$ cm^3 molecule^{-1} s^{-1} without added NO_2 compared to $(10.8 \pm 1.0) \times 10^{-11}$ with added NO_2 scavenger. The errors given are one standard deviation obtained from the data analysis. When estimates of systematic errors are included, the uncertainties should be increased to ±25% and one could argue that the difference between k_1 with and without added NO_2 is not significant. However, both experiments and numerical models show that the observed value of k_1 is very sensitive to small background concentrations of O and H atoms (see Figure 4). Moreover, addition of NO_2 in the present experiments consistently resulted in higher values of k_1. In the absence of any evidence that NO_2 chemistry interfered (see above), this suggests that values of k_1 near 7×10^{-11} cm^3 molecule^{-1} s^{-1} at room temperature are too low and that a better estimate is 11×10^{-11}.

The earlier studies recognized that reactions 6 and 7a could interfere with the measurement of k_1; background concentrations of both O and H atoms were monitored and found to be in the range 2×10^9 to 2×10^{10} cm^{-3}. Computer simulations which were based on the then accepted values for k_6 and k_{7a} indicated that OH regeneration from these reactions should not interfere.[10,12] If the atom concentrations were indeed below 5×10^9 cm^{-3}, simulations using the current higher rate constants show that reactions 6 and 7a should not have lowered observed k_1 by more than about 10%. However, these low atom concentrations are difficult to measure accurately, and realistic error limits on the concentrations are near ±50% to ±100%. Also, reactions 4 and 5 continuously generate O and H atoms in the OH source. Thus, it is possible that the minimum atom concentrations were nearer to 1×10^{10} cm^{-3} and interference from reactions 6 and 7a accounts for the difference between the earlier absolute studies and the present measurement with added NO_2.

Two of the previous low-pressure studies listed in Table IV were made relative to reaction 2.[10,11] These studies used the relation $k_1 = k_2[H_2O_2]/[HO_2]$, which is valid if $[HO_2]$ is at steady state and if reactions 1 and 2 are the major loss and source of HO_2, respectively. The average of the two studies is $(6.6 \pm 1.2) \times 10^{-11}$ cm^3 molecule^{-1} s^{-1}, which agrees with the absolute studies without added scavenger but is about 60% below the value of k_1 observed in the present study with NO_2 scavenger added. Corrections for HO_2 loss other than by reaction 1 lower the value of k_1 obtained. Thus, reactions 6 and 7a cannot account for the difference between these relative rate measurements and the present results. Sufficient details were not given to fully judge the accuracy of these studies; for example, it is important to know how good the steady-state approximation was in order to assess the size of any necessary corrections. This method requires knowledge of k_2 and absolute concentrations of both HO_2 and H_2O_2. It is likely that the combined errors in these parameters along with uncertainties in the steady-state $[HO_2]$ can account for the difference between these relative rate measurements and the present results.

Pressure Dependence. The present results with added scavenger agree well with the average value of $(1.2 \pm 0.4) \times 10^{-10}$ cm^3 molecule^{-1} s^{-1} obtained by previous measurements[13-19] near 1-atm total pressure. As pointed out earlier,[13] the k_1 pressure dependence observed between 75 and 730 Torr (see Introduction) lies well within the experimental error of the relative measurements and may not be significant. Agreement between the present results and the earlier high-pressure measurements shows that k_1 exhibits little or no pressure dependence between 1 and 1000 Torr.

Atmospheric Chemistry. The value of k_1 currently recommended for atmospheric models varies linearly from 7×10^{-11}

TABLE III: Reactions Used in Computer Simulations

no.	reaction	rate constant at 300 K[a]
1	$OH + HO_2 \rightarrow H_2O + O_2$	9.0×10^{-11} [b]
2	$OH + H_2O_2 \rightarrow HO_2 + H_2O$	1.7×10^{-12}
3	$HO_2 + HO_2 \rightarrow H_2O_2 + O_2$	1.7×10^{-12}
4	$OH + OH \rightarrow O + H_2O$	1.9×10^{-12}
5	$O + OH \rightarrow H + O_2$	3.3×10^{-11}
6	$O + HO_2 \rightarrow OH + O_2$	6.1×10^{-11} [c]
7a	$H + HO_2 \rightarrow OH + OH$	7.8×10^{-11} [d]
7b	$H + HO_2 \rightarrow O + H_2O$	2.0×10^{-12} [d]
7c	$H + HO_2 \rightarrow H_2 + O_2$	7.0×10^{-12} [d]
8	$F + H_2O \rightarrow OH + HF$	1.1×10^{-11} [e]
9	$O + NO_2 \rightarrow NO + O_2$	9.3×10^{-12}
10	$H + NO_2 \rightarrow OH + NO$	1.3×10^{-10}
11	$NO + HO_2 \rightarrow OH + NO_2$	8.3×10^{-12}
12	$F + H_2O_2 \rightarrow HO_2 + HF$	5.0×10^{-11} [e]
13	$OH + NO_2 + He \rightarrow HONO_2 + He$	9.2×10^{-31} [f]
14	$HO_2 + NO_2 + He \rightarrow HO_2NO_2 + He$	1.0×10^{-31} [f,g]
15	$OH + HONO_2 \rightarrow H_2O + NO_3$	1.0×10^{-13}
16	$OH + HO_2NO_2 \rightarrow$ products	4.6×10^{-12}
17	$OH + NO + He \rightarrow HONO + He$	3.8×10^{-31} [f]
18	$H + F_2 \rightarrow F + HF$	2.5×10^{-12} [h]
19	$F_2 + NO \rightarrow F + FNO$	1.5×10^{-14} [i]
20	$F + OH \rightarrow O + HF$	1.5×10^{-11} [j]
21	$F + HO_2 \rightarrow O_2 + HF$	4.0×10^{-11} [j]
22	$OH + wall \rightarrow$ products	5.0 s^{-1} [b]
23	$HO_2 + wall \rightarrow$ products	5.0 s^{-1} [b]

[a] Unless otherwise indicated, units are cm^3 molecule^{-1} s^{-1} and values were taken from ref 30–32. [b] Measured. [c] Reference 23. [d] Reference 24. [e] Reference 33. [f] In units of cm^6 molecule^{-2} s^{-1}. [g] References 34 and 35. [h] References 36 and 37. [i] Reference 38. [j] Reference 25.

TABLE IV: Summary of Recent k_1 Measurements at Low Pressure

$10^{11}k_1$, cm^3 molecule^{-1} s^{-1}	press., Torr	temp, K	method[a]	ref
(1.7 ± 0.5) exp[(416 ± 86)/T]	2.5	252–420	LIF, absolute study, [HO_2] ≫ [OH]	8
7.1 ± 1.2[b]	3	296	LIF, absolute study, [HO_2] ≫ [OH]	9
6.2 ± 2.3	1.6–10.4	295	LMR, absolute study, [HO_2] ≫ [OH]	10
6.9 ± 2.3	1.6	295	LMR, relative study, steady-state HO_2	10
6.2 ± 0.9[c]	2	298	LMR, relative study, steady-state HO_2	11
6.4 ± 1.5	1	299	RF, absolute study, [HO_2] ≫ [OH]	12
7.3 ± 1.0	1	299	RF, absolute study, [HO_2] ≫ [OH], no atom scavenger added	present study
10.8 ± 1.0	1	299	RF, NO_2 added to scavenge atoms	present study
(4.8 ± 0.8) exp[(250 ± 50)/T]	1	254–382	RF, NO_2 added to scavenge atoms	present study

[a] LIF = laser-induced fluorescence, LMR = laser magnetic resonance, RF = resonance fluorescence. [b] Corrected in ref 22. [c] Recalculated using $k_2 = 1.7 \times 10^{-12}$ cm^3 molecule^{-1} s^{-1}.

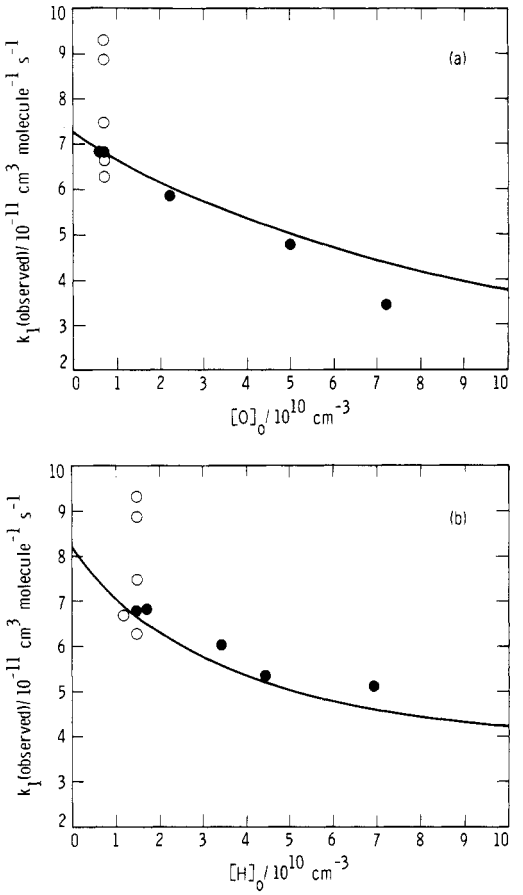

Figure 4. Plot of the observed rate constant, k_1, vs concentrations of (a) O atoms or (b) H atoms. Filled circles represent experiments in which atom concentrations were determined immediately following the k_1 measurements; for the open circles the atom concentrations were determined only at the end of a series of runs. The filled circles represent better controlled experiments and should be given more weight. The lines through the data are the result of a computer simulation. For the O atom plot (a), the background concentration of H atoms was 1.5×10^{10} cm^{-3}; for the H atom plot (b), the background concentration of O atoms was 8×10^9 cm^{-3}.

at low pressure to 12×10^{-11} cm^3 molecule^{-1} s^{-1} at 760 Torr.[30] The present results show that k_1 at low pressure is about 60% higher than previously thought and that its pressure dependence is considerably lower. In the upper atmosphere between 30 and 80 km, reaction 1 is the major loss of HO_x radicals. Over this region pressures range from about 10 to 0.01 Torr; and so, for the present discussion, any pressure dependence of k_1 is completely negligible. Table V compares k_1 obtained from the present results with the value currently recommended. Between 20 and 70 km use of the present results would increase calculated HO_x loss by 30–50%. Since current atmospheric models underestimate ozone concentrations by 30–80%, the higher HO_x loss would tend to bring predicted ozone concentrations into better agreement with observed values.[1]

TABLE V: Variation of k_1 in the Upper Atmosphere

altitude, km	T,[a] K	k_1 (present study)/ k_1 (previous value)[b]
20	217	1.30
25	222	1.31
30	227	1.35
35	237	1.40
40	250	1.45
45	264	1.51
50	271	1.53
55	261	1.49
60	247	1.44
65	233	1.39
70	220	1.33
75	208	1.27
80	198	1.22
85	189	1.17
90	187	1.17

[a] U.S. Standard Atmosphere (1976), middle latitudes. [b] Reference 30.

Summary. The absolute rate constant of the reaction OH + HO_2, k_1, was measured by using the discharge-flow resonance fluorescence technique with HO_2 in large excess. The measurements were carried out at 1-Torr total pressure and over the temperature range 254–382 K. Rate constants were obtained directly from observed decays of OH and measured concentrations of HO_2. The observed rate constant was independent of the type of reactor surface used. No significant difference was observed when F_2 or CF_4 was used as F atom precursors in the OH and HO_2 sources. Both experiments and computer simulations demonstrated that the observed value of k_1 is lowered by small concentrations of O and H atoms. At background atom concentra-

(30) DeMore, W. B.; Margitan, J. J.; Molina, M. J.; Watson, R. T.; Golden, D. M.; Hampson, R. F.; Kurylo, M. J.; Howard, C. J.; Ravishankara, A. R. Publication No. 85-37, 1985; Jet Propulsion Laboratory, California Institute of Technology, Pasadena, CA.

(31) Baulch, D. L.; Cox, R. A.; Hampson, R. F., Jr.; Kerr, J. A.; Troe, J.; Watson, R. T. *J. Phys. Chem. Ref. Data* **1984**, *13*, 1259.

(32) Hampson, R. F. Report No. FAA-EE-80-17, 1980; Federal Aviation Administration, Washington, D.C.

(33) Walther, C. D.; Wagner, H. Gg. *Ber. Bunsen-Ges. Phys. Chem.* **1983**, *87*, 403.

(34) Sander, S. P.; Peterson, M. E. *J. Phys. Chem.* **1984**, *88*, 1566.

(35) Howard, C. J. *J. Chem. Phys.* **1977**, *67*, 5258.

(36) Goldberg, I. B.; Schneider, G. R. *J. Chem. Phys.* **1976**, *65*, 147.

(37) Homann, K. H.; Schweinfurth, H.; Warnatz, J. *Ber. Bunsen-Ges. Phys. Chem.* **1977**, *81*, 724.

(38) Kolb, C. E. *J. Chem. Phys.* **1976**, *64*, 3087.

tions near 1×10^{10} cm^{-3}, observed $k_1 = (7.3 \pm 1.0) \times 10^{-11}$ cm^3 molecule^{-1} s^{-1} at 299 K; this result agrees with previous low-pressure measurements which give an average value of $(6.6 \pm 1.5) \times 10^{-11}$. When NO_2 was added to the reaction system in order to remove both atom species, observed values of k_1 increased to an average value of $(10.8 \pm 1.0) \times 10^{-11}$ cm^3 molecule^{-1} s^{-1} at 299 K. Computer simulations of the experiments with added NO_2 showed that reactions of OH and HO_2 with NO_2 (or with products produced when NO_2 was added) should not have increased the observed value of k_1. Previous measurements of k_1 near 1 atm average $(12 \pm 4) \times 10^{-11}$ cm^3 molecule^{-1} s^{-1} and agree well with the present results with added NO_2. This agreement suggests that k_1 exhibits no significant pressure dependence between 1 and 1000 Torr. Within error limits of one standard deviation, k_1 was found to increase slightly as the temperature was lowered. Over the temperature range studied, the data can be fit by using the Arrhenius expression $k_1 = (4.8 \pm 0.8) \times 10^{-11} \exp[(250 \pm 50)/T]$. However, within two standard deviations, the data can be fit to a temperature-independent value of $(10.8 \pm 2.8) \times 10^{-11}$. As a check for calibration errors, the rate constant for the reaction O + HO_2, k_6, was also determined in this study. The result of $(6.3 \pm 0.4) \times 10^{-11}$ cm^3 molecule^{-1} s^{-1} is in good agreement with the average value of $(5.7 \pm 0.5) \times 10^{-11}$ determined recently in this and other laboratories.[20-23]

Acknowledgment. The research described in this paper was performed at the Jet Propulsion Laboratory, California Institute of Technology, under contract with the National Aeronautics and Space Administration.

Registry No. OH, 3352-57-6; HO_2, 3170-83-0.

Study of Reactions of BH_3 with CO, NO, O_2, C_2H_4, and H_2O Using Diode Laser Absorption

L. Pasternack,* R. Jeffrey Balla,† and H. H. Nelson

Chemistry Division, Naval Research Laboratory, Code 6111, Washington, D.C. 20375-5000
(Received: July 6, 1987; In Final Form: September 21, 1987)

Absolute rate constants for the reaction of BH_3 with CO, NO, and C_2H_4 and upper limits for the reaction of BH_3 with O_2 and H_2O are reported. A diode laser is used to probe BH_3 disappearance. The reactions were studied at room temperature over a pressure range of 6–620 Torr with N_2 as a buffer gas. The rate constant for the association reaction of BH_3 + CO was found to be in the intermediate-pressure regime over the pressure range 10–620 Torr of N_2 with rate constants ranging from 1.5×10^{-13} to 47×10^{-13} cm^3 s^{-1}. For BH_3 + NO, the rate constant was found to approach the high-pressure limit of 3.7×10^{-13} cm^3 s^{-1} at pressures above $\simeq$200 Torr of N_2. The different rate constants and pressure dependences of this reaction compared to those of the BH_3 + CO reaction suggest a different mechanism. The pressure-independent rate constant ($P \geq 6$ Torr) for the reaction of BH_3 + C_2H_4 was found to be 5.2×10^{-11} cm^3 s^{-1}. The reactions of BH_3 + O_2 and BH_3 + H_2O were slower than could be measured in these experiments. Upper limits of 5×10^{-15} and 6×10^{-15} cm^3 s^{-1}, respectively, were placed on the rates of these reactions.

Introduction

There has been a resurgence of interest in the reactions of boranes due to the need to develop boron-assisted propellants. In studying the combustion of these systems, it has become evident that there is a lack of knowledge about basic chemical processes involving small boron-containing species.[1-3] Although several models for B/O/H and B/C/O/H combustion have been proposed,[2,4] there are still large uncertainties in the thermochemistry of key radicals in the models and very few rate constants have been measured.

In this paper we report rate constants from the measurement of BH_3 reactions with CO, NO, and C_2H_4 and upper limits for the rate constants for BH_3 reactions with O_2 and H_2O. There are no previous experimental measurements of the rates of these reactions, with the exception of $BH_3 + C_2H_4 \rightarrow H_2BC_2H_5$ which has been reported by Fehlner.[5] Several other elementary reactions of BH_3 have previously been studied in order to determine initial products and measure rate constants.[6] It has been found that, in general, BH_3 reactions proceed via adduct formation followed by rearrangement or elimination.[3]

We use a tunable diode laser as the probe source in a pump–probe experiment to study the kinetics of BH_3. The technique has been described previously.[7] BH_3 is formed by excimer laser photolysis (193 nm) of B_2H_6 as described by Irion and Kompa[8] and detected by IR absorption using a tunable diode laser at the frequency of a rotation line of the ν_2 vibration of BH_3.[9] We measure the rate of disappearance of BH_3 with added reactant gases.

Experimental Section

The reaction cell is a cylindrical Pyrex tube of 2-m length and 4-cm diameter with BaF_2 windows. The BH_3 radicals are pro-

†NRC/NRL Postdoctoral Research Associate. Current address: Morgantown Energy Technology Center, Morgantown, WV 26505.

(1) Bauer, S. H. In *Boron Chemistry*; Liebman, J. F., Williams, R., Eds., in press.
(2) Brown, R. C.; Kolb, C. E.; Yetter, R. A.; Dryer, F. L.; Rabitz, H. R. "Aerodyne Report ARI-RR-580", 1987.
(3) Fehlner, T. P.; Housecroft, C. E. In *Molecular Structure and Energetics*; Liebman, J. F.; Greenberg, A., Eds.; VCH: Deerfield Beach, FL, 1986; Vol. 1, Chapter 6.
(4) Shaub, W. M.; Lin, M. C. *NBS Spec. Publ. (U.S.)* **1979**, *No. 561*, 1249.
(5) Fehlner, T. P. *J. Am. Chem. Soc.* **1971**, *93*, 6366.
(6) Fehlner, T. P. *Int. J. Chem. Kinet.* **1975**, *7*, 633.
(7) Balla, R. J.; Pasternack, L. *J. Phys. Chem.* **1987**, *91*, 74.
(8) Irion, M. P.; Kompa, K. L. *J. Photochem.* **1986**, *32*, 139.
(9) Kawaguchi, K.; Butler, J. E.; Yamada, C.; Bauer, S. H.; Minowa, T.; Kanamori, H.; Hirota, E. *J. Chem. Phys.* **1987**, *87*, 2438.